

Dichroic behavior of multilayer structures based on anisotropically nanostructured silicon

J. Diener,^{a)} N. Künzner, D. Kovalev, E. Gross, and F. Koch
Physik-Department E16, Technische Universität München, D-85747 Garching, Germany

M. Fujii
Department of Electrical and Electronics Engineering, Faculty of Engineering, Kobe University, Rokkodai, Nada, Kobe 657-8501, Japan

(Received 17 December 2001; accepted for publication 27 February 2002)

Multilayer structures of anisotropically nanostructured (birefringent) silicon have been fabricated and studied by polarization-resolved reflection and transmission measurements. We demonstrate that stacks of birefringent porous silicon layers with alternating refractive indices and thicknesses act as dichroic Bragg reflectors or dichroic microcavities with a transmission/reflection dependent on the polarization direction of the incident light. The possibility of separate fine tuning of two orthogonally polarized transmission/reflection bands and their spectral splitting is demonstrated.

© 2002 American Institute of Physics. [DOI: 10.1063/1.1471581]

I. INTRODUCTION

During recent years, nanostructuring of semiconductors has been considered as an alternative way to search for new materials. Material properties, especially optical ones, can be modified by reducing the dimensions or by proper engineering of macroscopic structures on the nanometer scale. A key idea is the introduction of optical anisotropy due to the reduction of the symmetry of bulk crystals via ordered nanostructuring. The simplest approach based on drilling holes in semiconductors has proven to be an effective strategy for a variety of optical applications.¹⁻⁴ However, not all photonic applications require a strictly ordered distribution of holes. A quasiuniform distribution will be sufficient for specific applications under conditions when the dimensions of both holes and skeleton fragments are much smaller than the wavelength of the propagating light. Under these conditions the layers are optically homogeneous media where light propagates without internal scattering. The random spatial distribution of holes implies simply a reduced refractive index of the layers. Its value is defined by the fraction of empty space inside the layers.⁵ The easiest approach leading to dielectric nanostructuring is electrochemical etching of bulk semiconductor substrates resulting in their porous structures.

The porous modification of silicon [porous silicon (PSi)] consists of a sponge-like network of interconnected silicon (Si) nanocrystals. Due to the reduced size of Si nanocrystals and voids, in the range of a few nm, PSi is a quasicontinuous optical medium for the visible and infrared spectral range.

Another important property of porous silicon is the simplicity of controlling the mean refractive index of the layers and their thickness via variations of the etching current density and the time of etching, respectively.^{5,6} This enables modification of their dielectric properties in a controlled manner and production of a stack of alternating layers with

different refractive indices and thicknesses. A variety of PSi-based one-dimensional photonic structures like distributed Bragg reflectors (DBRs),^{7,8} microcavity resonators,⁹⁻¹¹ anti-reflection coatings,¹² and waveguides¹³ have been realized so far on the basis of this approach.

All these devices have been prepared from (100) oriented Si wafers. For this surface pores propagate preferentially along the direction of the current flow and the remaining Si nanocrystals are aligned along the [100] direction (perpendicular to the surface of the specimen).^{5,14} Consequently, PSi layers prepared from (100) Si wafers exhibit a dielectric in-plane isotropy.

A dielectric in-plane anisotropy can be achieved by changing the surface orientation of the Si wafer. The rate of pore propagation under electrochemical etching varies for different crystallographic orientations of Si wafers.⁵ Therefore a macroscopic alignment of the pores and remnant nanocrystals in a certain direction¹⁵ can be realized. Si due to its cubic lattice is not an anisotropic crystal but if the pores are formed to some extent ordered, the symmetry of the specimen can be changed and its porous modification becomes highly optically anisotropic due to anisotropic dielectric nanostructuring. For instance, PSi layers produced from (110) oriented Si wafers exhibit nanocrystal and pore elongation in the $[1\bar{1}0]$ surface plane direction.¹⁶ This macroscopic pore alignment has a very important implication for the optical properties of the layers. According to effective medium predictions this leads to a uniaxial surface symmetry with a refractive index $n_{[1\bar{1}0]}$ being different from $n_{[001]}$, where subscripts denote the polarization direction of the incident light. Indeed, as it has been demonstrated in Ref. 16 the value of the optical anisotropy achieved $n_{[1\bar{1}0]} - n_{[001]} = 0.25$ exceeds that of natural birefringent crystals.

We found the optical anisotropy of porous Si layers to be crucial for nonlinear wave interactions. The anisotropy level is high enough to compensate the normal dispersion of bulk Si and to achieve phase matching conditions for nonlinear

^{a)}Electronic mail: jdiener@physik.tu-muenchen.de

optical wave interactions.¹⁷ However, an ideal structure for nonlinear optical applications has to exhibit additionally light localization properties for the fundamental and higher harmonics of the propagating wave. For instance, a microcavity, consisting of a $\lambda/2$ layer placed between two distributed Bragg reflectors made from pairs of alternating $\lambda/4$ layers of high and low refractive indices acts as a multipass cell confining radiation and causing field enhancement inside. Therefore optical devices based on a stack of PSi layers acting as a microcavity (PSM) with each layer exhibiting an in-plane birefringence level which is high enough to achieve phase-matching conditions (i.e., having variation of the refractive index in three dimensions) seem to be almost ideal candidates for nonlinear optical interactions.

These structures yield optical effects which are difficult to achieve with conventional stacks of isotropic dielectrics. For instance, DBRs from anisotropically nanostructured (110) silicon have two distinct reflection bands depending on the polarization of the incident linearly polarized light.¹⁸ We study the optical properties of multiple in-plane optically anisotropic PSi layers in detail and demonstrate that porous silicon-based polarization-dependent dichroic Bragg reflectors and microcavities are promising for photonic applications of nanostructured Si in the visible and infrared spectral range.

This article is structured as follows: Section II deals with the sample preparation procedure and experimental details. Optical parameters of single optically anisotropic PSi layers and modeling of their optical properties are discussed in Sec. III. The possibility of fine spectral tuning of two orthogonally polarized reflection/transmission bands and their relative separation for DBRs is demonstrated in Sec. IV. Optical investigations of a dichroic (110) porous silicon microcavity are described in Sec. V.

II. EXPERIMENTAL DETAILS

PSi multilayer structures have been produced by electrochemical etching (in the dark) of (110) oriented *p*-type (Boron) doped Si wafers with a resistivity of 1.5 m Ω cm. The etching solution was a 1:1 (by volume) mixture of C₂H₅OH and concentrated aqueous HF acid (50%). For the preparation of the stacks two current densities were used: 22 mA/cm² ($=J_1$) and 70 mA/cm² ($=J_2$). To characterize single layer optical parameters separate layers etched with J_1 and J_2 have been prepared. Multilayer structures (ten J_1/J_2 cycles) were grown using etching at alternating low and high current densities (computer controlled current source) as schematically depicted in the upper left part of Fig. 1. A temporal variation of the etching current density results in a dielectric stack consisting of porous silicon layers having different thicknesses and average porosities. Actually, the etching procedure is identical to that one for PSi multilayers grown from (100) oriented Si wafers.¹⁹ In the upper right side of Fig. 1 we show the basic geometrical arrangement (in reflection geometry) and the crystallographic frame used. The surface of the sample is illuminated under almost normal incidence by unpolarized light from a halogen lamp. Reflected/transmitted light is analyzed by a Glan–Thomson

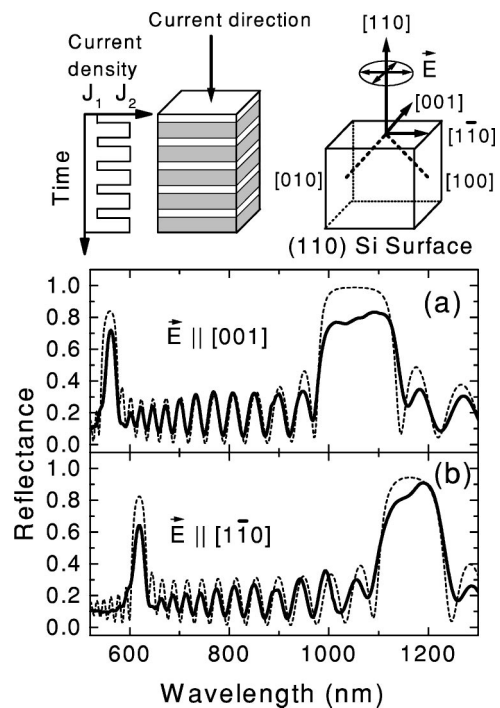


FIG. 1. The upper left part depicts the formation of multilayer structures from anisotropically nanostructured silicon. During the electrochemical etching of (110) oriented silicon wafers the etching current is periodically varied in time between low ($J_1=22$ mA/cm²) and high ($J_2=70$ mA/cm²) current density. This results in a dielectric stack with porous layers etched at J_1 (thickness d_1) and J_2 (thickness d_2). The upper right side illustrates the geometrical arrangement (in reflection geometry) and the used crystallographic frame. (a) and (b) The spectrally and polarization-resolved reflection of the same (110) distributed Bragg reflector ($d_1=95$ nm, $d_2=217$ nm). In (a) [(b)] the polarization vector of the reflected light (\vec{E}) is parallel to the [001] [$1\bar{1}0$] crystallographic directions in the (110) surface plane (solid lines). The dashed lines are results of calculations.

prism with polarization vector (\vec{E}) aligned either parallel to the [001] or to the [$1\bar{1}0$] crystallographic direction in the (110) surface plane. The polarized light was dispersed with a monochromator and detected with a charge coupled device (CCD). All spectra are normalized to the intensity of the incident light. Transmission measurements were performed with free-standing samples detached from the Si substrate by an electropolishing step. The specimens were fixed on a copper holder with a small pinhole (2 mm diameter). No noticeable difference has been observed when illuminating the specimen from the front or the back surface.

III. MEASURED AND CALCULATED OPTICAL PARAMETERS OF A SINGLE OPTICALLY ANISOTROPIC PSi LAYER

From spectrally and polarization-resolved measurements of reflection of linearly polarized light from a single (110) PSi layer prepared via etching with current densities J_1 or J_2 the corresponding refractive indices ($n_{[1\bar{1}0]}$ and $n_{[001]}$) and their anisotropy ($\Delta n = n_{[1\bar{1}0]} - n_{[001]}$) were evaluated. Their values are given in Table I. The in-plane optical anisotropy of the layers is evident: the refractive index for the electric field vector parallel to the [$1\bar{1}0$] crystallographic direction is substantially larger. As seen in the table, Δn varies for dif-

TABLE I. $n_{[001]}$ and $n_{[1\bar{1}0]}$ denote the measured refractive indices for single layers of (110) PSi etched with current densities J_1 and J_2 for different directions of \mathbf{E} with respect to the crystalline [001] and $[1\bar{1}0]$ directions. $F_{[001]}$ and $F_{[1\bar{1}0]}$ are the corresponding calculated Si volume filling factors (Bruggeman effective medium theory).

	$n_{[001]}$ ($\mathbf{E} \parallel [001]$)	$n_{[1\bar{1}0]}$ ($\mathbf{E} \parallel [1\bar{1}0]$)	Δn ($n_{[1\bar{1}0]} - n_{[001]}$)	$F_{[001]}$ (from $n_{[001]}$)	$F_{[1\bar{1}0]}$ (from $n_{[1\bar{1}0]}$)
J_1	2.39	2.55	0.16	42.2%	36.8%
J_2	1.55	1.75	0.2	70.5%	63.4%

ferent current densities (J_1 and J_2). This difference can be caused by the geometrical specifics of the standard etching geometry for (110) oriented Si wafers: the direction of the etching current flow is always normal to the (110) Si surface. While the etching in the [001] crystallographic direction is perpendicular to the current flow, the equivalent [010] and [100] directions have components parallel to the direction of the current. The etching rates parallel and perpendicular to the current direction are not equal and depend on the doping level of the substrate and the current density. Therefore the overall morphology of (110) PSi layers and consequently Δn depends on these two parameters. This is similar to the well studied microstructure formation of conventional (100) layers.^{5,6} This is in our opinion the reason for the difference between Δn values for (110) oriented PSi layers etched with J_1 and J_2 .

To correlate the porosities of the PSi layers and their refractive index values for (100) PSi layers the Bruggeman effective medium approximation has been successfully used.^{20,21} We found that similar to (100) PSi layers the absolute gravimetrically measured porosity (ρ) rises with increasing current density. However, for (110) PSi layers ρ is an average value and does not allow one to describe their anisotropic morphology.

A detailed description of the optical anisotropy parameters of a single PSi layer is crucial for the understanding of the overall spectral and polarization-dependent response of the multilayer structures. Therefore contrary to the ordinary Bruggeman model describing an isotropic medium, different volume filling factors F (volume fraction of empty space inside the layer) have been assumed to account for the polarization-dependent refractive index values. We used the simplified assumption that the (110) porous layers consist of dielectric spheres having different F for the two principal in-plane directions. Solving the equation:²¹

$$\sum_i F_i \left(\frac{\epsilon_i - \epsilon_{av}}{\epsilon_i + 2\epsilon_{av}} \right) = 0, \quad (1)$$

with F_i being the volume fraction of the i th medium (either Si or air), ϵ_i their dielectric constant, and ϵ_{av} the mean dielectric constant of the mixture, the two principal F values are calculated and given in the table. The spectral dispersion of the dielectric function of bulk Si leads to wavelength dependent values of $n_{[1\bar{1}0]}$, $n_{[001]}$, and Δn . Therefore the F values are evaluated in the near infrared region (at 1240 nm) where the refractive index of Si is almost dispersionless. For the calculation of the optical properties of (110) PSi single and multilayer systems in the visible spectral range the dis-

persion of the dielectric function of Si has been taken into account. Transmission and reflection spectra of the DBRs and PSMs are calculated applying the 2×2 transfer matrix method.²² The two principal values of the dielectric constant of (110) PSi at a given wavelength are determined with the Bruggeman formula [Eq. (1)] based on two different F values.

IV. DICHROIC BRAGG REFLECTORS

Figure 1 shows the spectra of the polarization-resolved reflection of a (110) DBR. Part (a) shows the spectrum of the reflected light being polarized parallel to the [001] crystallographic direction. In part (b) the polarization direction is along the $[1\bar{1}0]$ crystallographic direction. A DBR exhibits a high reflectivity band with the Bragg wavelength (λ_{Bragg}) approximately at its center. λ_{Bragg} depends on the thickness of the layers (d_1, d_2) and the corresponding refractive indices (n_1, n_2). The m th order of the Bragg peak is given by:²³

$$m\lambda_{\text{Bragg}} = 2(d_1 n_1 + d_2 n_2).$$

Contrary to (100) porous silicon DBRs⁸ the spectral position of $m\lambda_{\text{Bragg}}$ depends on the polarization direction of the incident light. For $\mathbf{E} \parallel [001]$ the first order Bragg band is centered around 1060 nm [Fig. 1(a)] while it is significantly shifted towards longer wavelength (~ 1170 nm) for $\mathbf{E} \parallel [1\bar{1}0]$ [Fig. 1(b)]. For high quality dichroic structures it is essential that both reflection bands do not overlap what is not the case for the first order Bragg reflection bands in Fig. 1. However, the second order bands in the visible spectral range are fully spectrally separated. The second order bands are twice narrower, as expected. The dispersion of the dielectric function of bulk Si leads to their spectral positions which are not exactly a half of the first order.

Dashed lines show reflectance spectra calculated on the basis of experimentally measured optical parameters of single layers. We found that for exact coincidence between the experimentally measured and calculated reflectance spectra a 10% correction of the filling factors towards higher values is required for thin layers etched with J_1 ($d < 150$ nm). This indicates that optical parameters of a thin single layer and those in a stack are slightly different. We believe that the reason for this is a very short etching time (shorter than 1 s) used to produce thin layers and a relatively slow response of the electrochemical reaction on the step-like switching of the current. After this correction the wavelength and the width of the first and second order Bragg bands are well reproduced by the calculations for both polar-

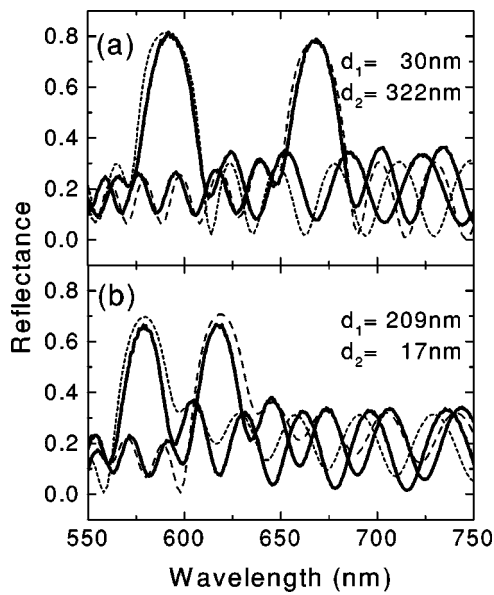


FIG. 2. The polarization-resolved reflection spectrum of two (110) distributed Bragg reflectors, having different spectral separation of the two orthogonally polarized reflection bands (solid lines). The reflection maximum at the high (low) energy side in (a) and (b) corresponds to the polarization vector of the reflected light parallel to the [001] ([110]) crystallographic directions in the (110) surface plane. d_1 (d_2) denotes the thickness of the layer etched with current density J_1 (J_2). Dashed lines are results of calculations.

ization directions (dashed lines in Fig. 1). The thicknesses used for the calculations ($d_{j_1}=95$ nm, $d_{j_2}=217$ nm) are within the range of estimates based on the etching time (approximately 90 and 200 nm).

The separation of the second order Bragg bands in Fig. 1 is 57 nm (618 nm for $\mathbf{E} \parallel [1\bar{1}0]$ and 561 nm for $\mathbf{E} \parallel [001]$) and is defined by the birefringence level (Δn) of each layer. The large variation of Δn , here around 20%, allows one to adjust the separation of the two reflection bands. By growing the thick layers with larger Δn (here at current density J_2) and thin layers with lower Δn the separation of the Bragg bands can be increased and vice versa.

Figure 2 shows two extreme cases. The relative thicknesses of the multilayers were intentionally chosen to achieve the appearance of the second order Bragg peaks in the same spectral range for both cases. In part (a) the layers with larger Δn are very thick and the separation from the second order Bragg bands is around 75 nm (668 nm for $\mathbf{E} \parallel [1\bar{1}0]$ and 593 nm for $\mathbf{E} \parallel [001]$). Part (b) of the same figure shows an example of a (110) DBR with the thick layers having low Δn . The corresponding wavelength difference between the reflection maxima is 38 nm (618 nm for $\mathbf{E} \parallel [1\bar{1}0]$ and 580 nm for $\mathbf{E} \parallel [001]$). The spectral separation of the Bragg bands is well reproduced by the calculations (dashed lines in Fig. 2). The estimated thicknesses (d_{j_1}/d_{j_2}) were 25 nm/310 nm [Fig. 2(a)] and 200 nm/15 nm [Fig. 2(b)] which are similar to the values used in the calculations (30 nm/322 nm and 209 nm/17 nm).

Figure 3 shows the polarization resolved reflection spectra of two (110) DBRs having nearly the same spectral separation but different spectral positions. The difference in the

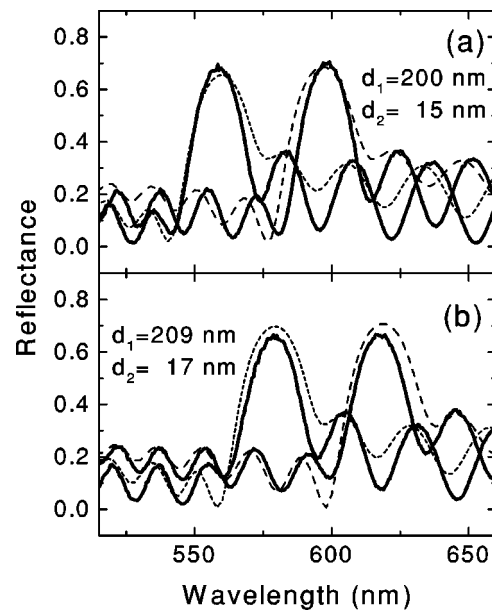


FIG. 3. Polarization-resolved reflection spectrum of two distinct (110) distributed Bragg reflectors having similar spectral separation of their two orthogonally polarized reflection bands but different wavelength positions (solid lines). The reflection maximum at the high (low) energy side in (a) and (b) corresponds to the polarization vector of the reflected light parallel to the [001] ([110]) crystallographic directions in the (110) surface plane. d_1 (d_2) denotes the thickness of the layer etched at current density J_1 (J_2). Dashed lines are calculated reflection spectra.

spectral position of the reflection bands is about 20 nm [Figs. 3(a) and 3(b)] while the separation of 40 nm [Fig. 3(a), 599 nm for $\mathbf{E} \parallel [1\bar{1}0]$ and 559 nm for $\mathbf{E} \parallel [001]$] and 38 nm [Fig. 3(b), 618 nm for $\mathbf{E} \parallel [1\bar{1}0]$ and 580 nm for $\mathbf{E} \parallel [001]$] are almost equal. It is clear that for a larger spectral shift (with the same separation interval) the thicknesses of both types of layers have to be carefully chosen taking into account the dispersion relation of bulk Si. Again, the predicted optical response (dashed lines) is in good agreement with experimental results.

As it follows from Figs. 2 and 3 with a proper choice of the thickness ratio and value of Δn it is possible to tune spectrally two orthogonally polarized reflection/transmission bands and adjust their spectral splitting separately. This is an additional degree of freedom and important for practical applications of dichroic photonic structures.

V. DICHROIC MICROCAVITIES

Another specific type of PSi multilayers are microcavities (PSMs) grown via electrochemical etching of Si wafers. PSMs are realized by inserting a layer with nd equal to $\lambda_{\text{PSM}}/2$ between two symmetric Bragg mirrors each one assembled from alternative layers having high and low refractive indices with $d_1 n_1 = d_2 n_2 = m \lambda_{\text{PSM}}/4$. The interference of the reflected waves of the two DBRs leads to a transmission maximum at λ_{PSM} within the spectral region of the high reflection (stop) band. Microcavities are of special interest for nonlinear or laser applications since the electric field of the light inside the central layer can be significantly enhanced.

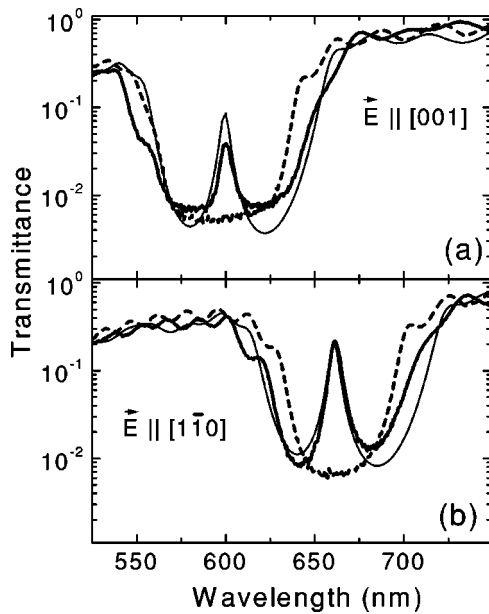


FIG. 4. Spectrally and polarization-resolved transmission through a (110) distributed Bragg reflector (dashed lines) and the corresponding (110) microcavity (thick solid lines). In (a) the polarization vector of the transmitted light (\mathbf{E}) is parallel to the [001] crystallographic directions in the (110) surface plane. (b) The same measurements for \mathbf{E} parallel to the $[1\bar{1}0]$ crystallographic directions in the (110) surface plane. Thin solid lines show calculated transmittance.

The basic requirement for PSMs are high quality DBRs. Figure 4 shows the transmission spectra of a free standing (110) DBR grown with 20 J_1/J_2 cycles (with thicknesses of 60 nm/90 nm) for the two principal polarization directions of the transmitted light (dashed lines). Since the suppression of the transmitted light for the first order Bragg peak is on the order of 99% and the edges of the stop bands are well pronounced the optical performance of the DBR is high.

A $\lambda_{\text{PSM}}/2$ layer has been introduced in an identical dielectric stack of layers by doubling of the etching time of the central layer. The thick solid lines in Fig. 4 show the polarization resolved transmission spectra of a (110) PSM. For both polarization directions a sharp cavity mode approximately in the center of the stop band can be seen. The finesse \hat{F} of a microcavity (or Fabry-Pèrot filter) is defined as the wavelength position of λ_{PSM} divided by the full width at half maximum of the cavity mode $\Delta\lambda$.²² For the PSM in Fig. 4 \hat{F} for light polarized in the $[1\bar{1}0]$ direction is $\lambda_{\text{PSM}}/\Delta\lambda = 661 \text{ nm}/7 \text{ nm} = 94.4$, which satisfies the requirements for optical grade quality. Due to the difference in Δn for different current densities the best performance of the DBRs can be achieved for one polarization direction only. To get the best optical quality DBRs usually $d_1 n_1$ is chosen to be equal to $d_2 n_2$ with a value of $m\lambda_{\text{PSM}}/4$. However, for (110) DBRs Δn is not the same for J_1 and J_2 (see Table I). Therefore this condition can only be fulfilled for one polarization direction. Since the PSM has been optimized for light polarized in the $[1\bar{1}0]$ direction, \hat{F} for light polarized in the [001] direction is smaller ($600 \text{ nm}/7 \text{ nm} = 85.7$). The intensities of the transmitted light differ as well. For the $[1\bar{1}0]$ polarization direction 22% of the initial light intensity is transmitted while it is

only 4% of the light polarized along the [001] crystallographic direction. The intensity of the transmitted light is limited by self-absorption in the PSi layers in this spectral range. For (100) mesoporous Si having 50% porosity the absorption coefficient at 660 nm is about 950 cm^{-1} ($\sim 1500 \text{ cm}^{-1}$ at 600 nm).^{24,25} For a given thickness of the PSM structure ($\sim 3\text{--}3.5 \mu\text{m}$) with an average porosity of $\sim 50\%$ up to 30% of the light is absorbed at 660 nm ($\sim 40\%$ at 600 nm).

Thin solid lines in Fig. 4 show the calculated transmittance for the PSM having thicknesses of 66 nm/99 nm. The position, the width, and the depth of the stop band, and the wavelength position of the cavity mode and its magnitude (especially for light polarized in the $[1\bar{1}0]$ crystallographic direction) are well reproduced by the fit. The field enhancement at 660 nm in the central layer of the (110) PSM for light polarized along the $[1\bar{1}0]$ crystallographic direction is estimated to be around 3. This value can be significantly enlarged by an increase of the dielectric contrast between the layers. Therefore thin (110) PSi layers having a larger variation of their average porosity and smaller interface roughness are desired and the preparation procedure still has to be improved. We note that all degrees of freedom for tuning the spectral position and the polarization state of the cavity mode are identical to those demonstrated for the DBRs.

VI. CONCLUSIONS

We demonstrate that stacks of (110) PSi layers, with each single layer having strong in-plane birefringence, can act as dichroic Bragg reflectors and microcavities. Due to the specifics of the crystallographic direction-selective etching process the strength of the birefringence depends strongly on the etching current density. This offers additional opportunities for the design of polarization-dependent optical PSi-based multilayered structures. We show that it is possible to tune spectrally two orthogonally polarized reflection/transmission bands of the PSi-based structures and adjust their spectral splitting separately. (110) PSi dichroic microcavities have been manufactured. Because the in-plane birefringence level is high enough to achieve phase-matching conditions for nonlinear wave interactions, microcavities prepared from (110) Si substrate seem to be promising candidates for a novel type of nonlinear optical media.

ACKNOWLEDGMENTS

The authors would like to acknowledge Deutsche Forschungsgemeinschaft for the support of this work. M. Fujii is grateful to the Alexander von Humboldt Foundation for financial support.

¹E. Yablonovitch, Phys. Rev. Lett. **58**, 2059 (1987).

²E. Yablonovitch and T. J. Gmitter, Phys. Rev. Lett. **63**, 1950 (1989).

³U. Grüning, V. Lehmann, and C. M. Engelhardt, Appl. Phys. Lett. **66**, 3254 (1995).

⁴F. Genereux, S. W. Leonhard, H. M. van Driel, A. Birner, and U. Gösele, Phys. Rev. B **63**, 161101(R) (2001).

⁵A. G. Cullis, L. T. Canham, and P. D. J. Calcott, J. Appl. Phys. **82**, 909 (1997).

⁶V. Lehmann, R. Stengl, and A. Luigart, Mater. Sci. Eng., B **69–70**, 11 (2000).

- ⁷G. Vincent, *Appl. Phys. Lett.* **64**, 2367 (1994).
- ⁸M. G. Berger, C. Dieker, M. Thönissen, L. Vescan, H. Lüth, H. Munder, W. Theiss, M. Wernke, and P. Grosse, *J. Phys. D* **27**, 1333 (1994).
- ⁹M. Araki, H. Koyama, and N. Koshida, *Appl. Phys. Lett.* **69**, 2956 (1996).
- ¹⁰C. Mazzoleni and L. Pavesi, *Appl. Phys. Lett.* **67**, 2983 (1996).
- ¹¹V. Mulloni and L. Pavesi, *Appl. Phys. Lett.* **76**, 2523 (2000).
- ¹²P. Menna, G. Di Francia, and V. La Ferrara, *Sol. Energy Mater. Sol. Cells* **37**, 13 (1995).
- ¹³H. F. Arrand, T. M. Benson, A. Loni, M. G. Krueger, M. Thönissen, and H. Lüth, *Electron. Lett.* **33**, 1724 (1997).
- ¹⁴M. Christophersen, J. Carstensen, and H. Föll, *Phys. Status Solidi A* **182**, 103 (2000).
- ¹⁵M. Christophersen, J. Carstensen, A. Feuerhake, and H. Föll, *Mater. Sci. Eng., B* **69–70**, 194 (2000).
- ¹⁶N. Künzner, D. Kovalev, J. Diener, E. Gross, V. Yu. Timoshenko, G. Polisski, F. Koch, and M. Fujii, *Opt. Lett.* **26**, 1265 (2001).
- ¹⁷L. A. Golovan, V. Yu. Timoshenko, A. B. Fedotov, L. P. Kuznetzova, D. A. Sidorov-Biryukov, P. K. Kashkarov, A. M. Zheltikov, D. Kovalev, N. Künzner, J. Diener, G. Polisski, and F. Koch, *Appl. Phys. B: Lasers Opt.* **73**, 31 (2001).
- ¹⁸J. Diener, N. Künzner, D. Kovalev, E. Gross, V. Yu. Timoshenko, G. Polisski, and F. Koch, *Appl. Phys. Lett.* **78**, 3887 (2001).
- ¹⁹O. Bisi, S. Ossicini, and L. Pavesi, *Surf. Sci. Rep.* **38**, 1 (2000).
- ²⁰D. A. G. Bruggeman, *Ann. Phys. (Paris)* **24**, 636 (1935).
- ²¹P. A. Snow, E. K. Squire, P. St. J. Russell, and L. T. Canham, *J. Appl. Phys.* **86**, 1781 (1999).
- ²²P. Yeh, *Optical Waves in Layered Media* (Wiley, New York, 1988), p. 102.
- ²³G. Björg, Y. Yamamoto, and H. Heitman, *Confined Electrons and Photons* (Plenum, New York, 1995), p. 481.
- ²⁴D. Kovalev, G. Polisski, M. Ben-Chorin, J. Diener, and F. Koch, *J. Appl. Phys.* **80**, 5978 (1996).
- ²⁵D. Kovalev, H. Heckler, G. Polisski, and F. Koch, *Phys. Status Solidi B* **215**, 871 (1999).